Journal of Sustainable Development of Smart Energy Networks

https://www.sdewes.org/jsdsen

Year 2026, Volume 1, Issue 4, 2030730

Original Research Article

A Framework for High-Resolution, Climate-Based Energy Time Series from EURO-CORDEX Climate Projections

***Matteo Buffo*[1*], *Fontina Petrakopoulou*[2], *Andrea Lazzaretto*[1]**

[1] Industrial Engineering Department, University of Padova, Via Venezia 1, 35121 Padova, Italy

[2] Chair of the Department of Energy Engineering and Climate Protection, Technische Universität Berlin, Marchstr. 18, 10587 Berlin, Germany

e-mail: mailto:matteo.buffo@studenti.unipd.it, andrea.lazzaretto@unipd.it, mailto:andrea.lazzaretto@unipd.it

Cite as: Buffo, M., Petrakopoulou, F., Lazzaretto, A., A Framework for High-Resolution, Climate-Based Energy Time Series from EURO-CORDEX Climate Projections, J. sustain. dev. smart. en. net., 1(4), 2030730, 2026, DOI: https://doi.org/10.13044/j.sdsen.d3.0730

ABSTRACT

Climate change is reshaping the environmental conditions of energy systems, increasing the need to integrate future climate information into energy modelling frameworks. This work presents a systematic, open-source framework for transforming regional climate projections into high-resolution, energy-relevant weather data. The pipeline processes EURO-CORDEX simulations to produce hourly time series for air temperature, solar irradiance, and wind speed, as well as daily precipitation, across Europe under multiple emission scenarios. In particular, it applies bias adjustment and temporal disaggregation to all variables except precipitation. A comprehensive evaluation against ERA5 is performed to assess dataset quality. Substantial biases in the raw projections are significantly reduced, and the resulting data realistically reproduce observed climate anomalies and the frequency of critical stress events, such as heatwaves and low-wind days. However, solar irradiance peaks are systematically underestimated due to temporal disaggregation to hourly resolution. Moreover, precipitation is deliberately excluded from bias adjustment, as uniform statistical correction degrades model performance. Despite these limitations, the framework provides a reproduceable approach for climate-aware energy system analysis, enabling the assessment of climate impacts on infrastructure planning and system adequacy. It also establishes a foundation for future work, including the integration of updated climate datasets, and the development of advanced post-processing techniques to improve the representation of variability and extremes.

KEYWORDS

Energy systems; Climate change; Weather time series; Climate models; Bias correction; Temporal disaggregations.

INTRODUCTION

The interdependence between climate and energy has intensely grown in recent decades. Energy infrastructure is both a major driver of human-driven climate change and one of the systems most vulnerable to its impacts. Rising global temperatures, increasing frequency of extreme weather events, fluctuating wind, solar irradiance, and precipitation patterns affect energy production, transmission, and demand. For instance, photovoltaic power output may decline due to temperature-induced reductions in cell efficiency and atmospheric phenomena that increase cloud cover [1]. Likewise, wind power generation can be influenced by shifts in

* Corresponding author

wind circulation patterns [2]. Periods of reduced precipitation may pose a threat to the output of hydropower plants and the cooling of thermoelectric facilities, resulting in lower efficiencies and disruptions [3]. On the demand side, space conditioning request will follow changing environmental conditions. Particularly, in Europe, heating demand is expected to decline in northern countries. Under a constant population scenario, this reduction will likely outweigh the projected rise in cooling demand in southern regions [4]. In addition, extended periods of low wind or solar radiation can cause critical stress in systems with high presence of intermittent renewable sources [5]. Thus, understanding how climate change may alter the frequency and persistence of such critical events is of fundamental importance, requiring access to climate data capable to represent the evolving conditions at scales relevant for energy systems.

The increasing need of high-resolution data, sufficiently reliable and relevant to energy applications, has driven the development of tailored datasets, designed to bridge the gap between climate science and energy system modelling [6]. As climate trajectories are linked to societal transition toward low carbon solutions and sustainable development, climate projections are widely used to assess impacts. These projections are generated using numerical global circulation models (GCMs), that divide the Earth into progressively smaller grid cells and simulate the climatic system by solving large sets of physical equations for the atmosphere, oceans, land, and ice, over sequential time steps. GCMs are run using radiative forcing trajectories that begin from preindustrial levels, follow observed historical values and are extended into the future according to prescribed scenarios of atmospheric greenhouse gas (GHG) concentrations, such as the Representative Concentration Pathways (RCPs) [7]. These scenarios, developed by the Intergovernmental Panel on Climate Changes (IPCC) [8], represent alternative trajectories of radiative forcing to the year 2100, corresponding to a specific mitigation ambition. Cumulated GHG concentrations act as a key external driver in climate model evolution, as they modify the energy balance of the atmosphere and drive temperature responses over time, which in turn interact with the oceans, cryosphere, and the other elements of the climate system. Model outputs, which are evaluated through intercomparison projects at the international level [9], inevitably contain biases, as they attempt to approximate the chaotic and non-linear nature of the climate system. These systematic deviations must be identified and, where possible, reduced using statistical post-processing methods and reliable historical databases to allow simulated variables to be calibrated against actual observations. Another major limitation concerns their spatiotemporal resolution, which is typically too coarse for direct use in energy-system applications. Energy system models generally require hourly (or sub-hourly) data to accurately represent the variability of renewable generation and demand, as well as high spatial resolution to capture local meteorological conditions. A third major limitation is the absence, in many climate projection databases, of key variables needed for energy applications. For example, wind speed is typically provided at 10 m above the ground rather than at turbine hub height, and direct normal irradiance (DNI), which is essential for concentrating solar technologies, is often not available.

In recent years, several initiatives have focused on energy-related data of future climate. Among these, the Copernicus Climate Change Service (C3S) [10] established a dedicated branch, C3S Energy [11], that developed the dataset “Climate and energy indicators for Europe from 2005 to 2100 derived from climate projections” [12]. Climate indicators, derived after the bias-adjustment of GCM projections, include 2 m air temperature, total precipitation, wind speed at 10 m and 100 m, and global horizontal irradiance (GHI). Energy indicators are obtained by feeding these climate variables into standard conversion models, supported by additional databases and probabilistic methods. The "Climate and energy related variables from the Pan-European Climate Database derived from reanalysis and climate projections” [13] provides similar outputs, at an enhanced spatiotemporal resolution. This database was obtained with statistical interpolation techniques applied to an ensemble of GCMs,

transformed from 3-hourly, 1° × 1° cells, to hourly, 0.25° × 0.25° cells, corresponding to approximately 30 km × 30 km. While these datasets, both available at the Climate Data Store (CDS) [14], represent a major advancement, the former still suffers from insufficient spatiotemporal resolution, and the latter relies on statistical interpolation of coarse climate information, which does not improve the representation of local features compared with physically consistent dynamical downscaling. Other datasets have instead tried to leverage climate projections more tailored to local scale applications, such as those developed inside the EURO-CORDEX project [15]. They are produced using a regional climate model (RCM) coupled to a driving GCM through a dynamical downscaling chain to increase the spatial resolution of final output, reaching 0.11° × 0.11°, approximately 12.5 km × 12.5 km. In practice, the GCM provides the general atmospheric conditions (wind components, temperature, specific humidity, pressure), which drive the higher-resolution RCM, that can freely develop detailed internal features at finer resolution. Climate projections generated in this way are used, for example, to create the SECURES-Met database [16], which provides bias-adjusted and hourly timeseries, aggregated at sub-national or provincial level. This database covers key variables such as 2 m air temperature, GHI and DNI, as well as normalized power output for wind and hydropower. Thus, it does not provide wind speed at 100 m and precipitation; instead it directly supplies end-use indicators, which are influenced by the specific underlying assumptions. Statistical temporal disaggregation is applied from daily projections to hourly outputs, and consequently limitations in capturing the intraday fluctuations of parameters are reported. A further contribution comes from another database that is explicitly designed to provide only climate parameters for energy system applications, rather than derived energy indicators [17]. This work uses 11 selected high-resolution EURO-CORDEX models which provide 3-hourly data to construct sub-ensembles. Focus is given on maintaining a low computational effort, a fundamental requirement when dealing with many models at high spatial and temporal resolutions. Projections are calibrated using reliable historical observations as well, but the temporal resolution remains limited to 3 hours, as no temporal disaggregation is applied, and the wind speed is still provided at 10 m.

Within this landscape, the present study introduces a systematic and computationally viable framework for processing high-resolution EURO-CORDEX projections to generate energy-relevant timeseries for the European domain that are bias-corrected, hourly, and flexibly spatially aggregated. Specifically, the projections are generated by the EC-Earth/RACMO model chain [18], [19], which has been identified as representative of a broader ensemble of climate models in terms of simulating annual mean temperature anomalies under different emission scenarios [16]. Although the use of ensembles of multiple climate models is generally recommended to better sample projection uncertainty, this work, motivated by an end-user perspective in the energy domain, prioritizes computational tractability and the delivery of a practical tool for direct time series application, and therefore relies on a single climate model. The dataset generated from this work provides hourly timeseries of 2 m air temperature, GHI, DNI, 10 m and 100 m wind speeds, together with daily precipitation, at a spatial resolution of up to 12.5 km × 12.5 km, representing the highest resolution currently available for downscaled future climate information over Europe. Users can select among three RCPs (corresponding to low-, medium-, and high-emission futures), enabling quantification of uncertainty associated with alternative long-term climate pathways. DNI and 100 m wind speed, which are not directly available in the original dataset, are derived through physically based formulations from GHI and 10 m wind speed, respectively. Finally, the study evaluates the resulting projected timeseries through comparison with the ERA5 dataset. The objectives are to assess the performance of the processing chain across the examined meteorological variables, identify any location-specific residual biases, evaluate the plausibility of simulated climate-change signals, and examine the ability to represent energy-relevant extreme events. Overall, the work aims to establish a robust methodological basis and provide a practical tool for climate-aware energy system analysis, by integrating

climate science, data processing and analytics, and energy system modelling within an interdisciplinary approach.

RESOURCES AND METHODS

The developed framework accounts for the weather variables with the greatest influence on energy supply and demand, while also considering their availability in major climate datasets. Surface air temperature is important for characterising the electricity demand driven by space conditioning in both summer and winter. It also affects the temperature of photovoltaic modules and the cooling water in thermoelectric power plants, thereby influencing their respective efficiencies [20], [21]. Global and direct solar irradiance determine the potential yield of photovoltaic and concentrating solar technologies, respectively. Wind speed determines the output of wind turbines through its cubic relationship with mechanical power. Finally, precipitation serves as a useful indicator for evaluating water availability in basins, which is needed for hydropower generation and for cooling in thermoelectric plants.

For the vertical extrapolation of wind speed at 100 m, for which only data at 10 m are available in the EURO-CORDEX projections database, a frequently used approximation of the logarithmic profile is adopted:

$$\frac{v(z)}{v(z_0)} = \left(\frac{z}{z_0}\right)^{\alpha} \tag{1}$$

where, $v(z)$ is the wind speed at height z, $v(z_0)$ the reference speed at height z_0 (here 10 m) and α an exponent accounting for the surface roughness effects.

To enhance accuracy, rather than adopting a spatially uniform α, this work constructs a uniform database, sampled on the projection model grid, using data from the Global Wind Atlas [22].

DNI is generated from GHI through the Erbs separation model [23] implemented with the "pvlib" Python library [24]:

$$\mathrm{DNI} = \frac{\mathrm{GHI} - \mathrm{DHI}}{cos\,\theta_z} \tag{2}$$

where, DHI is the diffuse horizontal irradiance, estimated using an empirical relationship that depends on the ratio of GHI to extraterrestrial irradiance, and θ_z is the solar zenith angle computed for each grid cell and time step.

Under near-horizontal sun conditions, DNI is set to zero to avoid numerical instabilities. Because variable derivation can introduce additional processing biases or amplify existing model errors, all derived variables are computed prior to statistical bias correction. This approach ensures that the correction targets the total bias affecting the final variable of interest.

The statistical bias correction uses the ERA5 reanalysis as a reference dataset [25]. ERA5 is a uniform-grid, high-resolution product generated by assimilating a large volume of observations into a numerical prediction system. Owing to its consistency and quality, it is widely used across multiple applications, including the energy sector [26], [27]. Within ERA5, wind speed at 100 m is directly available, while DNI can be derived from the field "Total sky direct solar radiation at surface", which represents the direct component on the horizontal plane, and corresponds to the term "GHI − DHI" in eq. (2).

Figure 1 shows the process to transform raw climate projections into bias-adjusted and hourly time series. The workflow is designed to produce datasets that are physically consistent and directly usable in energy system models while maintaining manageable computational requirements. Users can choose the desired RCP scenario (RCP 2.6, 4.5 or 8.5, corresponding to low-, medium- and high-emission pathways, respectively), the year (from 2006 to 2100), the

spatial area and the aggregation factor if a coarser resolution is needed. Climate projections are remotely retrieved from the CDS in NetCDF format, a commonly used format in the climate science field for storing multi-dimensional data. They are originally arranged on a rotated-pole grid. To enable comparison with ERA5 and facilitate their use in standard energy models, an initial re-gridding to a regular latitude-longitude grid is performed using the Python package "xESMF" [28]. This step restricts the spatial domain to 27° N and 70° N latitude, 12° W and 36° E longitude, as missing data near the boundaries could otherwise introduce larger mismatches during subsequent processing.

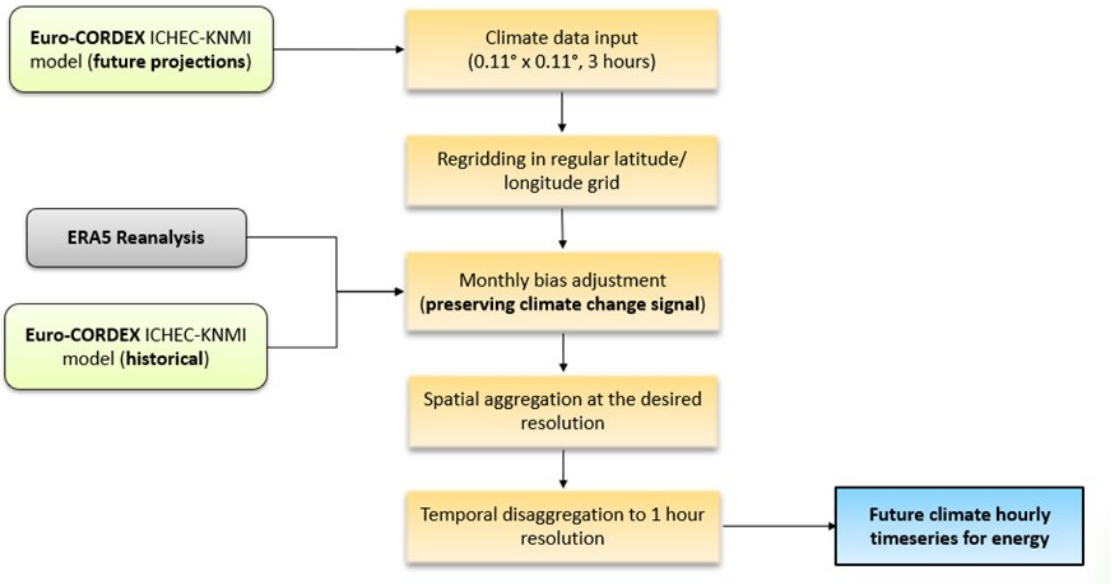

Figure 1. General data processing workflow

To quantify the systematic model biases targeted by the bias adjustment procedure, the historical simulation produced by the EC-Earth GCM and RACMO RCM chain is compared with the ERA5 reanalysis for winter and summer over the calibration period (1991–2005), after harmonizing their spatial and temporal resolutions (0.25° × 0.25°, 3-hourly, except for precipitation which is daily). At each grid cell p, bias is quantified as the mean difference between model and reference over the calibration period:

$$Bias(p) = \frac{1}{N}\sum_{n=1}^{N}(M_n(p) - R_n(p)) \quad (3)$$

where, M_n and R_n are the model and ERA5 reanalysis values at time index n, respectively, and N is the total number of samples.

The same calibration period is used for the subsequent adjustment, enabling a more robust treatment of short-term variability and internal climate variability. **Figure 2** shows the resulting mean bias for the relevant parameters. The most notable failures include a widespread cold bias in temperature, a marked overestimation of wind speed, further amplified by the extrapolation from 10 to 100 m, and the errors introduced by the derivation of DNI from GHI. Precipitation shows both localized positive and negative biases, strongly influenced by complex terrain and coastal regions. The resulting bias patterns are consistent with those reported by climate model developers [18], [19] and previous assessment studies [29].

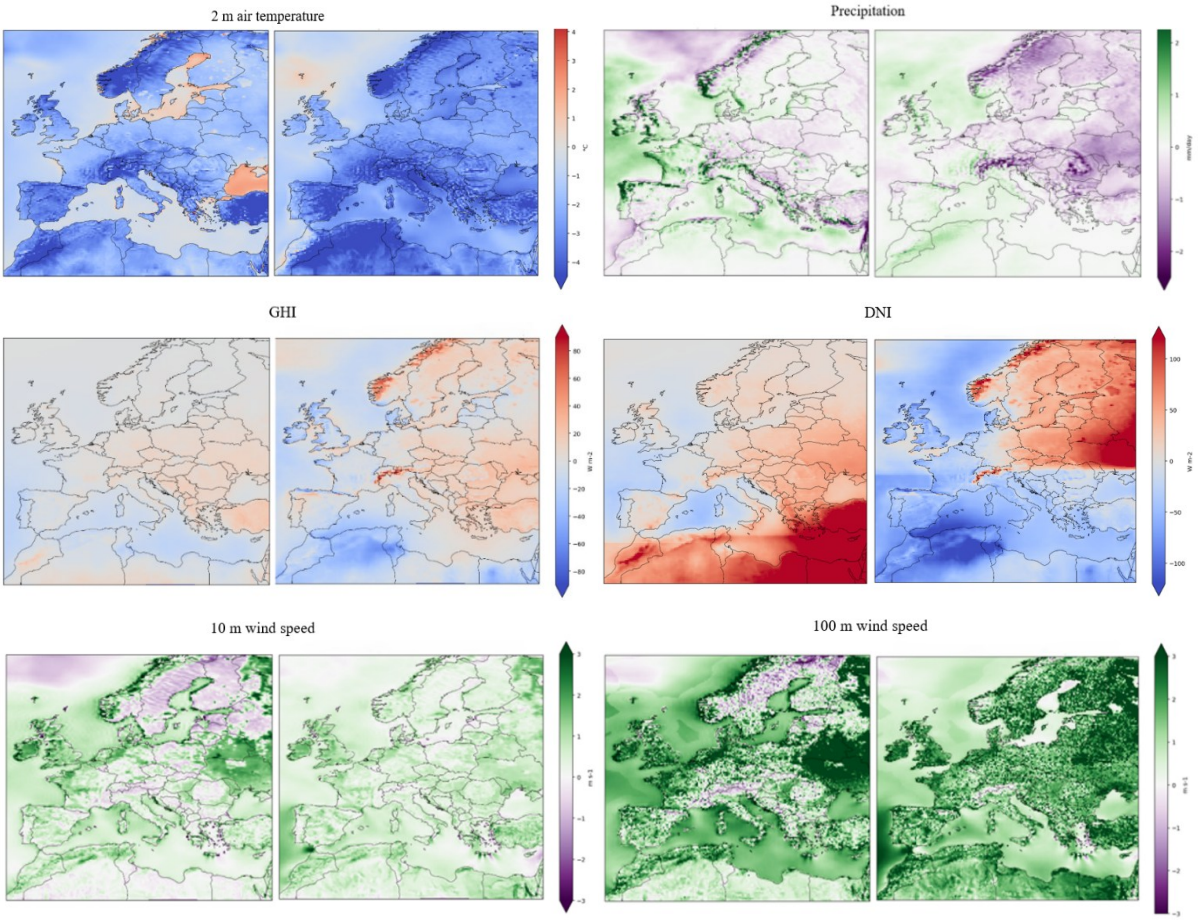

Figure 2. Mean bias of the relevant parameters over the period 1991-2005. For each parameter, the left panel shows winter (December, January, February) and the right panel shows summer (June, July, August)

Given the importance of preserving the climate change signal inherent in the projections [30], the bias adjustment strategy adopts the Quantile Delta Mapping (QDM) approach [31]. QDM operates in two key steps to correct the full statistical distribution of a variable while preserving the relative climate change signal between historical and future periods:

1. Historical calibration: a transfer function maps the quantiles of the historical model simulation to the corresponding quantiles of the historical reference (ERA5) data. This function corrects the model's statistical distribution (e.g., its mean, variance, and extremes) to match the observations, for the calibration period;
2. Future projection adjustment: before applying the historical calibration transfer function to the future projections, QDM calculates the relative change (delta) between the future and the historical model values at the same quantile, that is re-applied after the calibration.

Therefore, while the systematic bias is corrected, the simulated climate change is retained. The key underlying assumption is that the bias is stationary over time for each quantile. Mathematically, denoting $F_{\mathrm{m,c}}$ and $F_{\mathrm{o,c}}$ as the cumulative distribution functions (CDFs) of the historical raw model simulations and the ERA5 reanalysis, respectively, during the calibration period, and $F_{\mathrm{m,f}}$ as the CDF of the future raw projections $x_{\mathrm{m,f}}$, the corrected time series can be written as:

$$x_{\mathrm{corr}} = x_{\mathrm{m,f}} + [F_{\mathrm{o,c}}^{-1}(F_{\mathrm{m,f}}(x_{\mathrm{m,f}})) - F_{\mathrm{m,c}}^{-1}(F_{\mathrm{m,f}}(x_{\mathrm{m,f}}))] \quad (4)$$

for additive variables (e.g., temperature);

$$x_{\mathrm{corr}} = x_{\mathrm{m,f}} \times \frac{F_{\mathrm{o,c}}^{-1}(F_{\mathrm{m,f}}(x_{\mathrm{m,f}}))}{F_{\mathrm{m,c}}^{-1}(F_{\mathrm{m,f}}(x_{\mathrm{m,f}}))} \quad (5)$$

for variables that have zero as a lower boundary (e.g., wind speed and solar irradiance).

The practical implementation uses the "xsdba" sub-module of the Python package "xclim" [32]. Monthly correction functions are derived to account for the seasonal variations in bias. In this way, the distribution for each month of the projected year is adjusted using the historical distribution of the corresponding month, thereby avoiding cross-seasonal mixing of inputs. These correction functions are pre-computed by the "train" method of the QDM algorithm in the "xsdba" module and stored as serialized objects in NetCDF files. Subsequently, to correct any future projection period, the "adjust" method simply loads these pre-trained functions and applies them to the raw future model output. Access to the original historical time series is therefore not required for each adjustment step. This results in substantial savings in memory and computational cost (27 MB per function for the entire domain, compared with tens of GB needed to store the 15-year historical dataset) and enables very fast processing, typically within a few minutes.

Not all variables respond equally well to statistical correction. Precipitation, characterized by strong intermittency and stochastic variability, particularly at local scales, remains the most challenging variable to adjust. A tailored approach addressing both occurrence and intensity [33] led to degraded performance relative to the raw model output, regardless of whether monthly or annual calibration distributions were used. Consequently, precipitation was retained in its original form from the climate model.

Temporal disaggregation, from 3-hourly to hourly resolution is performed for temperature, solar irradiance and wind speed using a cubic spline interpolation, which captures most variability with limited computational cost. For solar irradiance, preservation of the diurnal cycle is ensured through a post-processing step that removes unphysical positive values occurring before sunrise and after sunset that may be introduced by interpolation. This is implemented via systematic comparison with "pvlib" clear-sky GHI, computed for each grid cell and time step and used as physical upper bound. To preliminarily evaluate the disaggregation performance, synthetic experiments were conducted using ERA5 hourly data aggregated to 3-hourly means and subsequently disaggregated back to hourly resolution using the cubic-spline method. The reconstructed series were compared to the original ERA5 data to evaluate the ability of the method to preserve peaks and represent sub-daily variability. Tests were performed over representative summer and winter weeks across multiple European climate regimes, using 0.50° x 0.50° spatial averaging to reduce single-point noise, showing accurate reproduction of temperature diurnal cycles and wind variability. However, daily irradiance peaks are systematically underestimated, indicating that the interpolation cannot fully capture midday maxima.

Table 1. Implementation details

Processing step	Resource	Settings
Regridding to regular lat-lon	xESMF	Method: bilinear; extrapolation: nearest_s2d; target grid: 0.11° × 0.11° regular (27°N–70°N, 12°W–36°E)
Wind speed vertical extrapolation	Global Wind Atlas (GWA)	α values pre-computed from GWA-extracted GeoTIFF maps of mean wind speed at 10 m and 100 m onto the 0.11° × 0.11° model grid
DNI derivation	pvlib	Erbs model: DNI computed from GHI and zenith angle; DNI set to zero where original GHI = 0; zenith pre-calculated via pvlib.Location.get_solarposition

Processing step	Resource	Settings
Bias asjustment	xsdba	QuantileDeltaMapping.train: differentiated between additive and multiplicative variables; original zeros preserved; one function per month, trained on the 1991-2005 period. QuantileDeltaMapping.adjust: constant extrapolation
Temporal disaggregation	xarray	Function interp, method: cubic; timestamp at the start of hour; values clipped: temperature ≥ 220 K, solar irradiance $\geq$ clear sky irradiance (calculated with pvlib library at each spatial cell and time, for avoiding eventual unphysical values before the actual sunrise or after the actual sunset, generated by the interpolation), wind speed ≥ 0;

RESULTS

The generated databases were evaluated through multiple tests. First, residual systematic deviations were quantified against the ERA5 reanalysis over an out-of-sample period. Second, the ability of the refined projections to reproduce the climate trends already observed in recent decades was examined. Finally, the capacity of the outputs to represent energy-relevant stress conditions was assessed in terms of the frequency of critical days. Overall, this comprehensive evaluation shows the quality of the proposed framework and supports the suitability of the refined projections as inputs for long-term energy system modelling.

Residual Biases

Hourly bias-reduced data were systematically checked across all grid points of the available domain against the ERA5 reanalysis in the period 2015-2024, using eq. (3) to compute the mean bias. This out-of-sample testing window is particularly suitable because it corresponds to a phase of increasing GHG forcing broadly comparable across all RCP scenarios [7], allowing the evaluation to focus on model performance rather than scenario-driven divergences. **Figure 3** presents spatial maps of the biases in the input projections alongside the residual biases after data refinement for the most relevant season of each variable, enabling visual comparison and a clear assessment of the added value.

The primary observation is that the out-of-sample comparison supports the assumption of bias stationarity under increased forcing conditions. In other words, the spatial bias patterns in the raw projections during the historical period (1991-2005, **Figure 2**) closely resemble those detected in the testing period (2015–2024, left panels of **Figure 3**). This supports the foundational assumption underlying the adopted bias adjustment methodology. Accordingly, confidence increases that the applied statistical correction is not substantially compromised by non-linear changes in model deviations under evolving climatic conditions.

The evaluation of near-surface air temperature indicates a substantial improvement. While the raw model, consistent with the historical bias assessment, displays a widespread cold bias exceeding -3 °C in many regions, the refined data reduce the residual bias to within ± 1.5 °C across the continent, and mostly within ± 1 °C. Wind speed at 100 m also shows substantial improvement. The extrapolated projections at 100 m, derived from 10 m wind speed, display deviations frequently approaching 3 $\mathrm{m \cdot s^{-1}}$ in the raw data, whereas the residual biases after refinements are strongly reduced to within ± 1 $\mathrm{m \cdot s^{-1}}$ across nearly the entire domain.

Temporal disaggregation does not introduce significant distortions for temperature or wind speed, owing to their relatively smooth diurnal cycles. In contrast, solar irradiance, often characterized by a sharp midday peak, exhibits domain-wide negative deviations, particularly in summer. These arise from the limited ability of the adopted disaggregation method to reproduce the true irradiance profile, thereby missing a significant fraction of the peak. The underestimation reaches about -50 $\mathrm{W \cdot m^{-2}}$ for GHI and up to -100 $\mathrm{W \cdot m^{-2}}$ for DNI, the latter being especially sensitive as then the initial projections were already affected by uncertainties associated with their empirical derivation using the Erbs model.

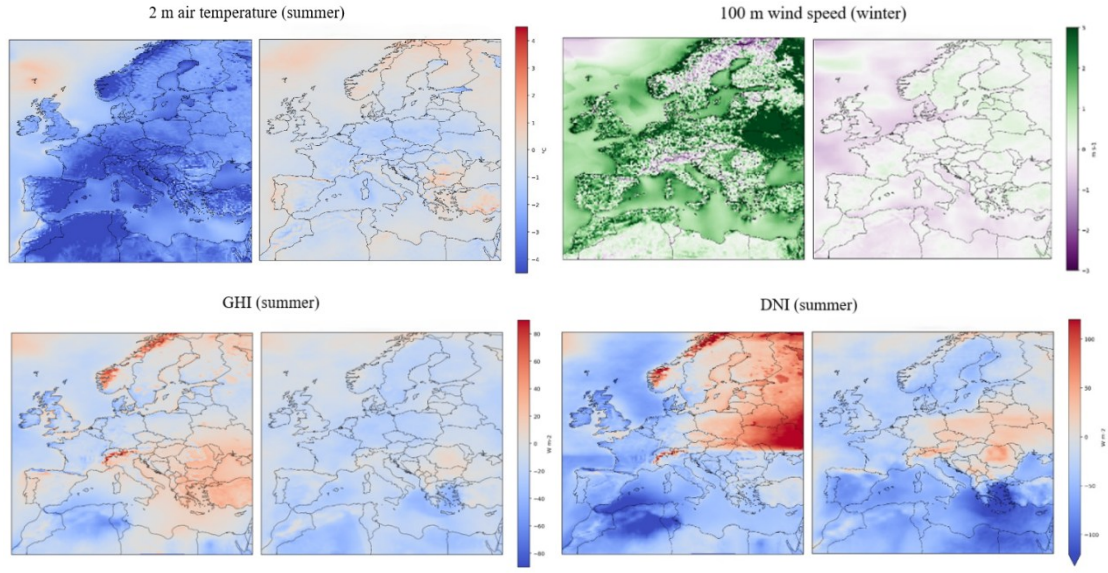

Figure 3. Mean bias for 2 m air temperature, 100 m wind speed and solar irradiance components, in the relevant seasons. For each variable, the left panel shows biases in the input projections, and the right panel shows residual biases after data refineme

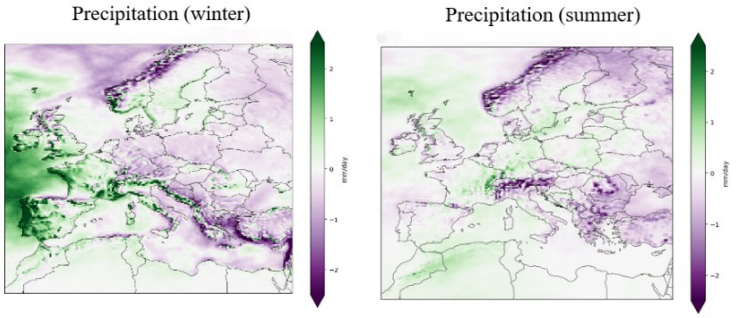

Figure 4. Mean bias for uncorrected daily precipitation, in winter and summer, evaluated over the period 2015-2024

Since precipitation was intentionally left unrefined, the spatial bias map for this variable (**Figure 4**) serves both as a diagnostic of raw model performance and as a reference for future improvements. Notably, in winter the spatial bias pattern evaluated over the testing period differs substantially from that observed in the historical assessment (**Figure 2**), which may partly explain the limited effectiveness of statistical bias correction for this highly variable and less predictable field. Pronounced positive biases, reaching up to $2\ \mathrm{mm} \cdot \mathrm{d}^{-1}$, are detected along the western European coasts and more widespread in the Alps, accompanied with underestimations in northern Europe and the eastern Mediterranean. By contrast, summer bias patterns show less change in the more recent evaluation, with significant deviations largely confined to mountainous regions.

Simulated Climate Anomalies

Consistency with observed climate trends is a fundamental aspect to assess in the context of ongoing climate change. Projected anomalies are defined for each variable as the difference between the mean value of the refined output over the 2015-2024 and the mean value of ERA5 data over the 1991-2000 reference period:

$$\mathrm{A}_{\mathrm{proj}}(x) = \mathrm{X}_{\mathrm{proj},2015-2024}(x) - \mathrm{X}_{\mathrm{ERA5},1991-2000}(x) \quad (6)$$

The resulting spatial distribution is then compared with the ERA5-observed anomaly map, computed over the same periods and used as the reference benchmark:

$$A_{proj}(x) = X_{ERA5,2015-2024}(x) - X_{ERA5,1991-2000}(x) \quad (7)$$

This comparison is presented in **Figure 5** for the most relevant season of each variable. The refined projections successfully reproduce the warming signal, generally between 1 °C and 2 °C, although some underestimation persists in central Europe due to residual cold bias. Wind speed anomalies, typically within $\pm 1\ m\ s^{-1}$, are reasonably represented, with broadly consistent spatial patterns except in northern regions. Anomaly analyses for GHI and DNI are not shown, as the artificial underestimation introduced by temporal disaggregation systematically distorts the results, producing negative anomalies that are not consistent with ERA5-observed trends.

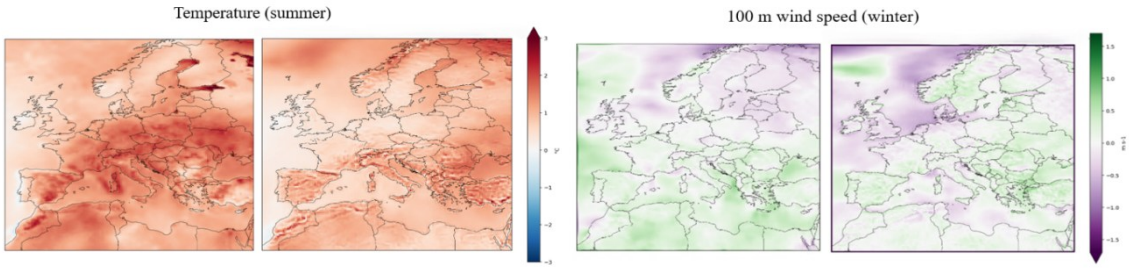

Figure 5. Climate anomalies (2015-2024 vs 1991-2000) for 2 m air temperature and 100 m wind speed in relevant seasons. For each variable, the left panel shows ERA5-observed anomaly, and the right panel shows the simulated anomaly derived from the refined

Finally, unrefined daily precipitation reproduces the spatial distribution of precipitation anomalies (in **Figure 6**) in a manner broadly consistent with observations across many regions, despite the aforementioned biases. In winter, ERA5 predominately shows increasing precipitation, particularly along the eastern coasts, Italy, and the Balkans. In summer observed patterns are more heterogenous, with positive anomalies in northern regions, and negative anomalies in the east. The projections tend to amplify both winter and summer signals, maintaining good qualitative agreement overall, except for inconsistent negative summer anomalies in the Alps and Scandinavia.

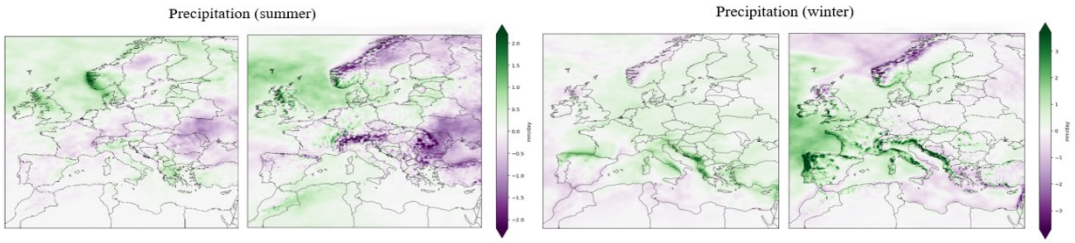

Figure 6. Climate anomalies (2015-2024 relative to 1991-2000) for uncorrected daily precipitation. For each season, the left panel shows ERA5-observed anomaly, and the right panel shows the simulated anomaly derived from the projections

Energy System Critical Stress Metrics

An essential requirement for the suitability of the proposed dataset for energy applications is the accurate replication of weather-driven critical stress events. Such events can significantly affect system reliability and the backup capacity needs, especially in systems with a growing share of variable renewable energy, while even firm generation may be exposed to water

availability constrains. Accordingly, a set of representative indicators for heat and cold waves, renewable energy droughts and water scarcity is defined. These are expressed as the mean annual frequency of critical days over the 2015-2024 period, based on selected thresholds in the corresponding meteorological variables. Consistent with the previous assessment, the results are compared with the same indicators derived from ERA5 data, as illustrated in **Figure 7**. To enhance the visualization of local impacts, critical days are aggregated at the NUTS-2 administrative level **[34]** for EU countries, while for other territories and marine areas they are kept at the native spatial resolution.

Heat waves, associated with high cooling demand, are identified as summer days with $T_{max} > 35\,°C$, a threshold commonly used to indicate stress conditions for the grid. These events occur more frequently over the central and southern Iberian Peninsula, with a notable presence also in parts of Italy, the Balkans, and western Anatolia. The refined data reproduce this spatial pattern realistically, with slight but largely unavoidable underestimation. By contrast, the original projections severely underrepresent such events due to the pronounced cold bias. Very cold winter days (with $T_{min} < -5\,°C$) are also assessed, as such temperatures often correspond to peak heating demand. They occur most often in the Alps, Scandinavia, and more broadly across eastern Europe, where the refined dataset tends to show some overestimation. Nevertheless, the agreement with observations is substantially improved relative to raw projections, which are systematically shifted toward lower temperatures.

To assess potential energy droughts, both low-wind and low-irradiance days were considered. However, only the former are presented, as the known negative bias in solar irradiance would likely lead to an overestimation of poor sunlight conditions. Low-wind days are evaluated for winter and defined as days with $v(100)_{max} < 5\,\mathrm{m\,s^{-1}}$, corresponding approximately to the cut-in speed for many wind turbines, and, in any case, indicative of very low generation potential. The highest frequencies occur over Italy, the Balkans and Turkey, with secondary maxima in Spain, southern France and parts of central-eastern Europe. The spatial distribution derived from the proposed dataset shows very strong agreement with ERA5.

Finally, winter days with negligible precipitation ($\text{daily total} < 0.1\,\mathrm{mm}$, indicating effectively dry conditions) are evaluated, noting that this meteorological variable is used directly from the climate model output. Such dry days occur most frequently in Mediterranean regions, especially over northern Africa and southern Spain. The projections show noticeable underestimation in these areas, on the order of 5-10 days, while the overall spatial pattern remains broadly consistent across most other regions.

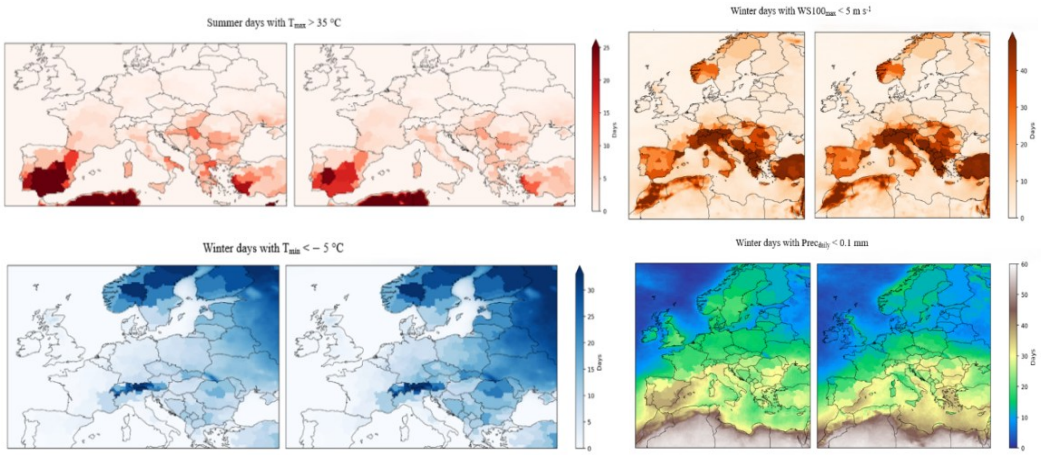

Figure 7. Mean annual number of potential weather-induced critical days for the energy system, based on selected thresholds. For each impact indicator, the left panel shows ERA5-observed frequency, and the right panel shows the simulated frequency derived from the provided dataset, both evaluated over the period 2015-2024

Overall, these assessments demonstrate the reliability of the proposed long-term dataset. The results indicate robust performance for temperature and wind speed, while solar irradiance retains notable limitations. Precipitation projections also exhibit some inaccuracies, which are typical for this highly stochastic variable.

DISCUSSION

The methodological framework developed in this work is designed to enable use of long-term climate information for energy system modellers, addressing the persistent gap between raw climate projection outputs and the need for weather data at fine spatiotemporal resolution. The resulting tool spans a broad European domain and extends to the end of the century, allowing users to explore alternative climatic futures under different socioeconomic pathways. The dataset provides physically consistent projections of future weather conditions at a scale suitable for deriving a wide range of energy system implications. This capacity is particularly valuable for long-term planning and operational assessments. Climate change is, in fact, one of the major global factors threatening energy system resilience, and effective adaptation measures require robust and credible quantitative inputs.

In addition, the proposed tool is readily upgradeable and can be enhanced over time across all processing stages. A notable strength is its operational simplicity and speed, despite the methodological complexity, which lowers the barrier to accessing climate data that would otherwise require substantial programming and climate model expertise. The framework also provides flexibility through the option to aggregate outputs to coarser spatial scales. This enables the dataset to support both localized and large-scale analyses, while keeping computational costs and data volumes manageable. However, excessively strong spatial aggregation should be avoided, as it inevitably degrades the fidelity of local weather signals.

Overall, the work confirms several challenges widely reported in the literature, while offering practical responses through the careful selection, implementation, and coordination of well-established techniques in climate-energy research. The adopted methodology relies entirely on physically based models and peer-reviewed statistical procedures, while adapting the treatment to the specific characteristics of each variable, including seasonal variability and diurnal behaviour. The achieved spatiotemporal resolution is among the highest currently available, compared with similar resources in the literature. By leveraging EURO-CORDEX downscaled sub-daily inputs, this requirement is readily met for variables directly available in the climate database, such as temperature. In contrast, the derivation of key parameters not included in the original dataset proves more challenging. The estimation of wind speed at heights representative of turbine hubs constitutes a particularly valuable component of the workflow and represents a major improvement in terms of physical consistency and bias reduction. Conversely, the derivation of DNI using the Erbs model exhibits non-negligible accuracy limitations, especially in regions where this variable is most critical, namely southern Europe. As a result, DNI estimation requires more advanced treatment, since bias adjustment alone cannot fully compensate for deficiencies in the initial empirical deviation. Ideally, an improved approach should explicitly incorporate projected changes in cloud cover, which may evolve differently from historical conditions and directly affect the performance of concentrating solar technologies.

The monthly QDM adjustment explicitly accounts for the pronounced seasonal variability of temperature, solar irradiance and wind speed. This feature is particularly important for applications in which seasonality strongly influences demand patterns and renewable generation. Because biases were found to vary by season (**Figure 2**), applying a uniform year-round correction would degrade performance. In contrast, the monthly approach achieves effective bias reduction in both summer and winter. From an end-user perspective, this refined dataset provides more reliable estimates for variables that directly affect simulated power flows and system adequacy, although some residual biases remain in specific regions

(**Figure 3**). These are partly attributable to the subsequent temporal disaggregation step, which intentionally avoids more complex and computationally intensive methods in order to preserve overall tool efficiency. While the final time series are satisfactory for temperature and wind speed, solar irradiance remains affected by a systematic underestimation of daily peak values. Further methodological development is therefore required to identify optimal strategies for accurately reproducing irradiance peaks throughout the year, as the present hourly output is not recommended for peak-sensitive applications. One potential mitigation strategy is to apply a post-processing method based on the clear-sky index, to improve the reconstruction of the irradiance profile during daily peak hours.

Moreover, the current version of the framework does not apply bias correction to precipitation, as initial tests did not yield substantial improvements when implemented uniformly across the full domain. Precipitation is highly intermittent and strongly controlled by local convective processes, which are difficult to correct using spatially homogenous statistical methods. Although providing unadjusted daily precipitation does not invalidate the usefulness of this variable (provided that its biases are explicitly acknowledged, as shown in **Figure 4**), future work should prioritize the refinement of precipitation treatment and bias reduction strategies. Region-specific statistical correction approaches, for example, may offer a more effective pathway. A further consideration, particularly relevant for hydropower and thermal plant cooling, is that the proposed database captures only precipitation changes, and therefore cannot fully represent the broader hydrological impacts of climate change. Future alterations will be not only limited to rainfall patterns, but will also involve changes in river regimes and basins characteristics, partly driven by the ongoing Alpine glacier retreat. Major European rivers including the Po, Rhine, Rhone, and several Danube tributaries, originate in glaciated regions. Consequently, glacier-related changes are likely to affect their long-term water availability and the basins they supply. This has important implications for power plants generation and cooling, potentially affecting even dispatchable capacity that is critical for system reliability. A more comprehensive integration of long-term hydrological and cryospheric projections is therefore increasingly necessary to fully capture the dynamics of the water-energy nexus.

Alongside this research direction, the present framework opens a wide range of additional evaluation and development opportunities. Because the assessment also examined the capability to identify energy-relevant extreme events under present-day warming conditions, similar analysis can be extended to future periods to quantify the increasing influence of critical stresses under different scenarios. In combination with complementary datasets, the proposed tool may support further studies, such as projections of increased maintenance costs associated with higher summer operational temperatures, availability reductions in dispatchable units under tightening hydrological constraints, and evolving spatiotemporal patterns of energy droughts driven by prolonged and concurrent shortages of solar and wind resources. Another important research avenue concerns the post-processing of long-term weather time series to enable their efficient integration into computationally tractable yet robust energy system models. Because such models often rely on representative days or typical years, multi-annual time series must typically be reduced using clustering techniques. Climate-aware clustering strategies are therefore needed to ensure that representative periods preserve projected climatic variability and the increasing frequency of extreme events, thereby avoiding systematic smoothing of critical conditions.

The outlined results and future developments are supported by a strong emphasis on transparency and reproducibility, enabling continuous improvement and broad applicability. The full implementation of the proposed framework has been developed in Python and is publicly available. The complete codebase, including all scripts required to retrieve, process, bias-adjust, and temporarily disaggregate climate projections, is hosted in a dedicated online repository **[35]**. The repository also includes the required library dependencies, auxiliary datasets for wind speed extrapolation and bias correction, and detailed execution guidelines.

User interaction is intentionally limited to a small set of clearly defined inputs, such as scenario selection, time horizon, geographical domain, and variables of interest. All processing steps are fully automated within a modular workflow, ensuring methodological consistency across different user configurations. Data processing relies exclusively on widely used libraries within the climate and energy modelling communities. The code can be executed on any modern operating system with at least 8 GB of RAM and does not require specialized hardware. Typical runtimes are on the order of a few minutes per variable, largely driven by data retrieval and bias adjustment. The resulting outputs are provided in standardized NetCDF format with complete metadata.

CONCLUSION

This work established a coherent, reproducible, and updatable pathway for transforming regional climate projections into energy system-tailored weather data. By processing EURO-CORDEX climate simulations through a structured workflow, it delivers a novel dataset of hourly, bias-adjusted weather variables tailored for European energy applications through the end of the century. The developed workflow comprises remote data retrieval, re-gridding to a standard latitude-longitude grid, physical derivation of wind speed at 100 m and DNI (not available in the original dataset), monthly bias adjustment using Quantile Delta Mapping calibrated against the ERA5 reanalysis, and temporal disaggregation to hourly resolution. Precipitation remains the only variable provided unadjusted and at daily resolution. Overall, the framework maintains manageable computational requirements by leveraging pre-computed, reusable components and efficient coordination of processing steps.

The refined time series demonstrate clear improvements over raw climate model outputs and provide valuable insights into how future climatic conditions may influence energy systems. The 2 m air temperature, originally affected by a cold bias exceeding -3 °C across much of Europe, is corrected to within ± 1.5 °C almost everywhere. Similarly, the strong overestimation in derived 100 m wind speed, often reaching 3 m s^{-1}, is substantially reduced, with residual errors well below ± 1 m s^{-1}. Solar irradiance, including both GHI and derived DNI, also benefits from bias adjustment. However, a widespread underestimation of daily peak values persists, particularly in summer, reaching approximately -50 W m^{-2} for GHI and up to -100 W m^{-2} for DNI in Mediterranean areas. This limitation is primarily attributable to the adopted temporal disaggregation, which is unable to fully capture midday maxima. In contrast, temperature and wind speed are not substantially degraded by this step. Uncorrected precipitation exhibits acceptable performance overall, despite localized biases near mountainous and coastal areas. The consistency of simulated climate anomalies between the 2015-2024 and 1991-2000 periods is also satisfactory, with the warming signal reasonably reproduced, albeit slightly attenuated in central Europe. Wind speed and precipitation trends are broadly consistent as well. Energy-relevant critical stress events are also reasonably captured, with the refined outputs providing credible estimates of hot waves, cold spells, low-wind conditions, and dry days, despite some deviations linked to residual biases.

Overall, these results demonstrate that the proposed processing workflow significantly enhances the usefulness of climate projections for long-term energy planning. Although some limitations remain, they do not compromise the overall robustness of the framework but instead point to clear priorities for future development, with the modular architecture and reproducibility of the tool facilitating further upgrades. At the same time, the framework highlights the need for climate-aware clustering methodologies and for more integrated approaches that couple climate projections with hydrological and cryospheric models.

As climate change continues to alter the environmental context in which energy systems operate, the present approach represents a substantial step toward deeper and more accurate integration of climate information into long-term energy system design and operation.

NOMENCLATURE

Symbols

F	Cumulative distribution function (CDF)	[-]
$M_n(p)$	Model value at time step n and in cell p	
$R_n(p)$	ERA5 reanalysis value at time step n and in cell p	
$v(z)$	Wind speed at height z	[m/s]
$X_{ERA5,1991-2000}$ (x)	Mean value of ERA5 reanalysis over the 1991-2000 period	
$X_{ERA5,2015-2024}$(x)	Mean value of ERA5 reanalysis over the 2015-2024 period	
$X_{proj,2015-2024}$(x)	Mean value of the refined output over the 2015-2024 period	

Greek letters

α	Surface roughness exponent	[-]
θ_z	Solar zenith angle	[°]

Abbreviations

C3S	Copernicus Climate Change Service	
CDS	Climate Data Store	
DHI	Diffuse Horizontal Irradiance	[W/m^2]
DNI	Direct Normal Irradiance	[W/m^2]
ERA5	The fifth generation ECMWF atmospheric reanalysis of the global climate (1940 – present)	
GCM	Global Circulation Model	
GHG	Greenhouse Gas	
GHI	Global Horizontal Irradiance	[W/m^2]
NetCDF	Network Common Data Form	
RCM	Regional Climate Model	
RCP	Representative Concentration Pathway	
QDM	Quantile Delta Mapping	

REFERENCES

1. Jerez, S., Tobin, I., Vautard, R., Montávez, J. P., López-Romero, J. M., Thais, F., Bartók, B., Christensen, O. B., Colette, A., Déqué, M., Nikulin, G., Kotlarski, S., van Meijgaard, E., Teichmann, C. & Wild, M., The impact of climate change on photovoltaic power generation in Europe, *Nat. Commun.*, Vol. 6, 10014, 2015, https://doi.org/10.1038/ncomms10014.
2. Tobin, I., Jerez, S., Vautard, R., Thais, F., van Meijgaard, E., Prein, A., Déqué, M., Kotlarski, S., Fox Maule, C., Nikulin, G., Noël, T. & Teichmann, C., Climate change impacts on the power generation potential of a European mid-century wind farms scenario, *Environmental Research Letters*, Vol. 11, 034013, 2016, https://doi.org/10.1088/1748-9326/11/3/034013.
3. Petrakopoulou, F., Robinson, A. & Olmeda-Delgado, M., Impact of climate change on fossil fuel power-plant efficiency and water use, *Journal of Cleaner Production*, Vol. 273, 122816, 2020, https://doi.org/10.1016/j.jclepro.2020.122816.
4. Damm, A., Köberl, J., Prettenthaler, F., Rogler, N. & Töglhofer, C., Impacts of +2°C global warming on electricity demand in Europe, *Climate Services*, Vol. 7, pp 12-30, 2016, https://doi.org/10.1016/j.cliser.2016.07.001.
5. Van der Wiel, K., Stoop, L. P., van Zuijlen, B.R.H., Blackport, R., van den Broek, M.A. & Selten, F.M., Meteorological Conditions Leading to Extreme Low Variable Renewable Energy Production and Extreme High Energy Shortfall, *Renewable and Sustainable Energy Reviews*, Vol. 111, pp 261-275, 2019, https://doi.org/10.1016/j.rser.2019.04.065.

6. Craig, M. T., Wohland, J., Stoop, L. P., Kies, A., Pickering, B., Bloomfield, H. C., Browell, J., De Felice, M., Dent, C. J., Deroubaix, A., Frischmuth, F., Gonzalez, P. L. M., Grochowicz, A., Gruber, K., Härtel, P., Kittel, M., Kotzur, L., Labuhn, I., Lundquist, J. K., Pflugradt, N., van der Wiel, K., Zeyringer, M. & Brayshaw, D. J., Overcoming the disconnect between energy system and climate modeling, *Joule*, Vol. 6, No. 7, pp 1405-1417, 2022, https://doi.org/10.1016/j.joule.2022.05.010.
7. Meinshausen, M., Smith, S. J., Calvin, K., Daniel, J. S., Kainuma, M. L. T., Lamarque, J.-F., Matsumoto, K., Montzka, S. A., Raper, S. C. B., Riahi, K., Thomson, A., Velders, G. J. M. & van Vuuren, D. P. P., The RCP Greenhouse Gas Concentrations and Their Extensions from 1765 to 2300, Climatic Change, Vol. 109, No. 1, 213, 2011, https://doi.org/10.1007/s10584-011-0156-z.
8. Edenhofer, O., Pichs-Madruga, R., Sokona, Y., Farahani, E., Kadner, S., Seyboth, K., Adler, A., Baum, I., Brunner, S., Eickemeier, P., Kriemann, B., Savolainen, J., Schlömer, S., von Stechow, C., Zwickel, T. & Minx, J. C. (eds.), Climate Change 2014: Mitigation of Climate Change. Contribution of Working Group III to the Fifth Assessment Report of the Intergovernmental Panel on Climate Change, Report, Cambridge University Press, Cambridge, United Kingdom and New York, NY, USA, 2014.
9. Eyring, V., Bony, S., Meehl, G. A., Senior, C. A., Stevens, B., Stouffer, R. J., Taylor, K. E., Overview of the Coupled Model Intercomparison Project Phase 6 (CMIP6) experimental design and organization, *Geosci. Model Dev.*, Vol. 9, No. 5, pp 1937–1958, https://doi.org/10.5194/gmd-9-1937-2016, 2016.
10. Thépaut, J.-N., Pinty, B. & Dee, D., The Copernicus programme and its climate change service, *Proceedings of IEEE International Geoscience and Remote Sensing Symposium*, Valencia, Spain, pp 1591-1593, July 2018, https://doi.org/10.1109/IGARSS.2018.8518067.
11. Dubus, L., Saint-Drenan, Y.-M., Troccoli, A., De Felice, M., Moreau, Y., Ho-Tran, L., Goodess, C., Amaro e Silva, R. & Sanger, L., C3S Energy: A climate service for the provision of power supply and demand indicators for Europe based on the ERA5 reanalysis and ENTSO-E data, *Meteorological Applications*, Vol. 30, No. 5, e2145, 2023, https://doi.org/10.1002/met.2145.
12. Troccoli, A., Sanger, L., Goodess, C., Ogonji, J., Dubus, L., Vautard F., Pons, R., Jin, X., Levavasseur, G., Legrand, R., Grigis, L., Martinoni-Lapierre, S., Viel, C., Parey, S., Oueslati, B., Saint-Drenan, Y.-M., Mendes, J., Osborne, J. & Guentchev, G., Climate and energy indicators for Europe datasets: Technical description of methodologies followed in the development of each product, Technical Report, ECMWF, 2023.
13. Troccoli, A., Borga, M., Zaramella, M., Lusito, L., Cordeddu, S., Restivo, E., Aldrigo, G., Campostrini, S., Strada, S., Saint-Drenan, Y.-M., Amaro, R., Koivisto, M., Olsen, B. & Kanellas, P., Climate and energy related variables from the Pan-European Climate Database derived from reanalysis and climate projections v4.2: Product user guide (PUG), Technical Report, ECMWF, 2023.
14. Raoult, B., Bergeron, C., López Alós, A., Thépaut, J.-N. & Dee, D., Climate service develops user-friendly data store, *ECMWF Newsletter*, Vol. 151, pp 22-27, 2017, https://doi.org/10.21957/p3c285.
    Datasets available from: https://cds.climate.copernicus.eu/, [Accessed: Feb. 26, 2026].
15. Jacob, D., Petersen, J., Eggert, B., Alias, A., Bøssing Christensen, O., Bouwer, L. M., Braun, A., Colette, A., Déqué, M., Georgievski, G., Georgopoulou, E., Gobiet, A., Menut, L., Nikulin, G., Haensler, A., Hempelmann, N., Jones, C., Keuler, K., Kovats, S., Kröner, N., Kotlarski, S., Kriegsmann, A., Martin, E., Van Meijgaard, E., Moseley, C., Pfeifer, S., Preuschmann, S., Radermacher, C., Radtke, K., Rechid, D., Rounsevell, M., Samuelsson, P., Somot, S., Soussana, J.-F., Teichmann, C., Valentini, R., Vautard, R., Weber, B. & Yiou, P., EURO-CORDEX: new high-resolution climate change projections for European impact research, *Regional Environmental Change*, Vol. 14, No. 2, pp 563-578, 2014, https://doi.org/10.1007/s10113-013-0499-2.

16. Formayer, H., Nadeem, I., Leidinger, D., Maier, P., Schöniger, F., Suna, D., Resch, G., Totschnig, G. & Lehner, F., SECURES-Met: A European meteorological data set suitable for electricity modelling applications, *Scientific Data*, Vol. 10, 590, 2023, https://doi.org/10.1038/s41597-023-02494-4.
17. Bartók, B., Tobin, I., Vautard, R., Vrac, M., Jin, X., Levavasseur, G., Denvil, S., Dubus, L., Parey, S., Michelangeli, P.-A., Troccoli, A. & Saint-Drenan, Y.-M., A climate projection dataset tailored for the European energy sector, *Climate Services*, Vol. 16, 100138, 2019, https://doi.org/10.1016/j.cliser.2019.100138.
18. Hazeleger, W., Wang, X., Severijns, C., Ştefănescu, S., Bintanja, R., Sterl, A., Wyser, K., Semmler, T., Yang, S., Van den Hurk, B., Van Noije, T., van der Linden, E. & van der Wiel, K., EC-Earth V2.2: description and validation of a new seamless earth system prediction model, *Climate Dynamics*, Vol. 39, pp 2611-2629, 2012, https://doi.org/10.1007/s00382-011-1228-5.
19. van Meijgaard, E., van Ulft, L. H., Lenderink, G., de Roode, S. R., Wipfler, E. L., Boers, R., & van Timmermans, R. M. A., Refinement and application of a regional atmospheric model for climate scenario calculations of western Europe, Technical Report, KvR 054/12, National Research Program Climate Changes Spatial Planning, Nieuwegein, Netherlands, 2012.
20. Radziemska, E., The effect of temperature on the power drop in crystalline silicon solar cells, *Renewable Energy*, Vol. 28, No. 1, pp 1-12, 2003, https://doi.org/10.1016/S0960-1481(02)00015-0.
21. Morrill, J. C., Bales, R. C. & Conklin, M. H., Estimating Stream Temperature from Air Temperature: Implications for Future Water Quality, *Journal of Environmental Engineering*, Vol. 131, No. 1, pp 139-146, 2005, https://doi.org/10.1061/(ASCE)0733-9372(2005)131:1(139).
22. Davis, N. N., Badger, J., Hahmann, A. N., Hansen, B. O., Mortensen, N. G., Kelly, M., Larsén, X. G., Olsen, B. T., Floors, R., Lizcano, G., Casso, P., Lacave, O., Bosch, A., Bauwens, I., Knight, O. J., Potter van Loon, A., Fox, R., Parvanyan, T., Krohn Hansen, S. B., Heathfield, D., Onninen, M. & Drummond, R., The Global Wind Atlas: A High-Resolution Dataset of Climatologies and Associated Web-Based Application, *Bulletin of the American Meteorological Society*, Vol. 104, No. 8, pp E1507-E1525, 2023, https://doi.org/10.1175/BAMS-D-21-0075.1.
Dataset available from: https://globalwindatlas.info, [Accessed: Feb. 26, 2026].
23. Erbs, D. G., Klein, S. A. & Duffie, J. A., Estimation of the diffuse radiation fraction for hourly, daily and monthly average global radiation, *Solar Energy*, Vol. 28, No. 4, pp 293-302, 1982, https://doi.org/10.1016/0038-092X(82)90302-4.
24. Holmgren, W., Anderson, K., Hansen, C., Wandrews, R., Jensen, A. R., Mikofski, M., Daxini, R., Lorenzo, A., Luis, E., Krien, U., Driesse, A., Stark, C., Sánchez de León Peque, M., Transue, T., Sifnaios, I., Rhee, K., Priyadarshi, N., Boeman, L., Guo, V., Anoma, M. A., Miller, E., Stein, J., Aneja, S., Nicolau, B. & Vining, W., pvlib/pvlib-python: v0.13.0, *Zenodo*, 2025, https://doi.org/10.5281/zenodo.15614720.
25. Hersbach, H., Bell, B., Berrisford, P., Hirahara, S., Horányi, A., Muñoz-Sabater, J., Nicolas, J., Peubey, C., Radu, R., Schepers, D., Simmons, A., Soci, C., Abdalla, S., Abellan, X., Balsamo, G., Bechtold, P., Biavati, G., Bidlot, J., Bonavita, M., De Chiara, G., Dahlgren, P., Dee, D., Diamantakis, M., Dragani, R., Flemming, J., Forbes, R., Fuentes, M., Geer, A., Haimberger, L., Healy, S., Hogan, R. J., Hólm, E., Janisková, M., Keeley, S., Laloyaux, P., Lopez, P., Lupu, C., Radnoti, G., De Rosnay, P., Rozum, I., Vamborg, F., Villaume, S. & Thépaut, J.-N., The ERA5 global reanalysis, *Quarterly Journal of the Royal Meteorological Society*, Vol. 146, pp 1999-2049, 2020, https://doi.org/10.1002/qj.3803.
26. Olauson, J., ERA5: The new champion of wind power modelling?, *Renewable Energy*, Vol. 126, pp 322-331, 2018, https://doi.org/10.1016/j.renene.2018.03.056.

27. Urraca, R., Huld, T., Gracia Amillo, A., Martinez-De-Pison, F., Kaspar, F. & Sanz-Garcia, A., Evaluation of global horizontal irradiance estimates from ERA5 and COSMOREA6 reanalyses using ground and satellite-based data, *Solar Energy*, Vol. 164, pp 339-354, 2018, https://doi.org/10.1016/j.solener.2018.02.059.
28. Zhuang, J., Dussin, R., Huard, D., Bourgault, P., Banihirwe, A., Raynaud, S., Malevich, B., Schupfner, M., Levang, S., Jüling, A., Almansi, M., Rondeau, G., Rasp, S., Smith, T. J., Stachelek, J., Plough, M., Bell, R. and Li, X., pangeo-data/xESMF: v0.7.1, *Zenodo*, 2023, https://doi.org/10.5281/zenodo.7800141.
29. Kotlarski, S., Keuler, K., Christensen, O. B., Colette, A., Déqué, M., Gobiet, A., Goergen, K., Jacob, D., Lüthi, D., van Meijgaard, E., Nikulin, G., Schär, C., Teichmann, C., Vautard, R., Warrach-Sagi, K. & Wulfmeyer, V., Regional climate modeling on European scales: a joint standard evaluation of the EURO-CORDEX RCM ensemble, *Geoscientific Model Development*, Vol. 7, No. 4, pp 1297-1333, 2014, https://doi.org/10.5194/gmd-7-1297-2014.
30. Maraun, D. & Widmann, M., Statistical Downscaling and Bias Correction for Climate Research, Cambridge University Press, Cambridge, United Kingdom, 2018.
31. Lehner, F., Nadeem, I. & Formayer, H., Evaluating skills and issues of quantile-based bias adjustment for climate change scenarios, *Advances in Statistical Climatology, Meteorology and Oceanography*, Vol. 9, No. 1, pp 29-44, 2023, https://doi.org/10.5194/ascmo-9-29-2023.
32. Bourgault, P., Huard, D., Smith, T. J., Logan, T., Aoun, A., Lavoie, J., Dupuis, É., Rondeau-Genesse, G., *et al.*, xclim: xarray-based climate data analytics (v0.59.0). *Zenodo*, 2025, https://doi.org/10.5281/zenodo.17487243.
33. Vrac, M., Noël, T. & Vautard, R., Bias correction of precipitation through Singularity Stochastic Removal: Because occurrences matter, *Journal of Geophysical Research: Atmospheres*, Vol. 121, No. 10, pp 5237-5258, 2016, https://doi.org/10.1002/2015JD024511.
34. Nomenclature of Territorial Units for Statistics (NUTS), Eurostat, Luxembourg, 1995.
35. Buffo, M., Framework-EURO-CORDEX-to-hourly-bias-adjusted-timeseries-for-energy, *GitHub* repository, 2025, https://github.com/matteobuffo01/Framework-EURO-CORDEX-to-hourly-bias-adjusted-timeseries-for-energy, [Accessed: Feb. 26, 2026].

Paper submitted: 27.02.2026
Paper revised: 23.04.2026
Paper accepted: 28.04.2026

Fontina Petrakopoulou is Editorial Board Member of *Journal of Sustainable Development of Smart Energy Networks*. The editorial handling of this article was conducted independently of author's role on the Editorial Board. The manuscript was handled independently by another editor, with the above-mentioned Editorial Board member excluded from the initial assessment, reviewer selection, peer-review evaluation, and decision-making, and with no relevant competing interests.